CrossMark

Grain boundary wetting transition in Al–Mg alloys

B.B. Straumal[a,b,c,*], O.A. Kogtenkova[a], M.Yu. Murashkin[d], M.F. Bulatov[e], T. Czeppe[f], P. Zięba[f]

[a] Institute of Solid State Physics, Russian Academy of Sciences, Ac. Ossipyan Str. 2, 142432 Chernogolovka, Russia
[b] Karlsruhe Institute of Technology (KIT), Institute of Nanotechnology, Hermann-von-Helmholtz-Platz 1, 76344 Eggenstein-Leopoldshafen, Germany
[c] Laboratory of Hybrid Nanomaterials, National University of Science and Technology "MISIS", Leninskii Prosp. 4, 119049 Moscow, Russia
[d] Institute for Physics of Advanced Materials, Ufa State Aviation Technical University, K. Marx Str. 12, 450000 Ufa, Russia
[e] Moscow Technological University (MIREA), 78 Vernadsky Avenue, 119454 Moscow, Russia
[f] Institute of Metallurgy and Materials Science, Polish Academy of Sciences, 25 Reymonta Street, 30-059 Krakow, Poland

ARTICLE INFO

ABSTRACT

The melting of coarse- and fine-grained Al–Mg alloys was studied by the differential scanning calorimetry (DSC). The transition from incomplete to complete wetting of grain boundaries (GBs) takes place in binary Al–Mg alloys. The heat effect of GB wetting manifests itself in the asymmetric shape of the DSC melting curve. By decreasing grain size (and increasing specific area of GBs) the GB "shoulder" in DSC curve becomes more pronounced. Basing on DSC data, the position of GB solidus (or premelting) line for Al–Mg alloys has been estimated. Contrary to the Al–Zn alloys, the difference between bulk and GB solidus does not exceed 2 °C.
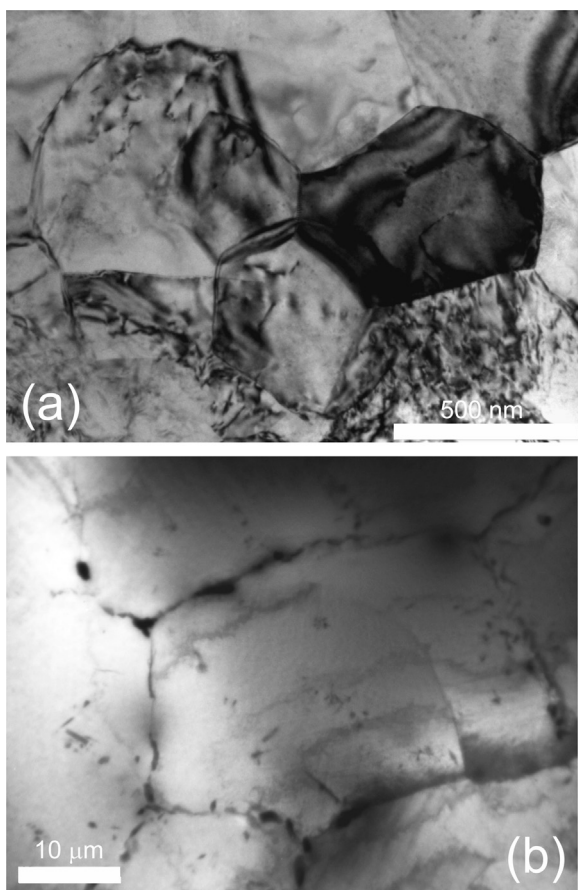
1. Introduction

The Al–Mg alloys play an important role in the technology of light alloys due to their high strength and ductility [1]. It is possible to further improve the mechanical properties of Al–Mg alloys by tailoring their grain size and, consequently, the specific area of grain boundaries (GBs) [2–7]. The transition from incomplete to complete wetting of Al/Al GBs by the melt or by the second solid phase Al_3Mg_2 has been observed recently in the Al–Mg alloys [8–11]. A GB is completely wetted if the contact angle between GB and second phase is zero. In this case second phase has to substitute a GB separating both grains by a continuous layer. A GB is incompletely wetted if the contact angle between GB and the second phase is finite. In this case the GB can exist in the equilibrium contact with the second phase. Cahn and Ebner and Saam first demonstrated that the (reversible) transition from incomplete to complete wetting is a true surface phase transformation [12,13]. Later the wetting phase transitions were observed also in GBs (see [8,9,14,15] and references therein).

Already Cahn predicted that if the tie-line of the wetting phase transition is present in the two-phase area of a phase diagram, this tie-line cannot finish at the border between two-phase and one-phase areas (called solidus, solvus or transus) [12]. The wetting tie-line should continue in a single-phase area of a phase diagram as a line of so-called prewetting phase transition [12]. Later the continuation of

wetting tie-lines into single-phase area and resulting formation of thin GB layers of a second phase (called also GB complexions) found a focused attention both of experimentalists and theoreticians (for review see [14,16–27]).

The influence of such GB layers on various properties of polycrystals is especially pronounced in the micro-, submicro- and nano-grained materials [28]. Very promising techniques to obtain the bulk nanograined materials are the different variants of severe plastic deformation (SPD). Such SPD techniques as equal channel angular pressing (ECAP) and high-pressure torsion (HPT) do not involve changes in the sample geometry and permit to strain a material without its fracture. In our previous works SPD of binary Al–Zn, Al–Mg and ternary Al–Zn–Mg alloys has been studied [2,29–31]. It has been demonstrated that during HPT, the supersaturated solid solution of Zn in Al decomposes completely and closely approaches the equilibrium state corresponding to the room temperature. As a result, the thin GB layers of Zn-rich phase form in Al–Zn polycrystals and lead to the very high room-temperature ductility [28,32]. The processes of structural changes during SPD are very complicated and have not been yet fully understood [33–36]. Differential scanning calorimetry (DSC) permitted us to observe the GB solidus line ~10–25 °C below the bulk solidus line in binary Al–Zn and Cu–Co alloys [37,38]. However, the GB solidus line was not visible in ternary Al–Zn–Mg alloys [39]. Therefore, the DSC investigation of GB wetting phase transition in the Al–Mg system before and after HPT is the goal of this work.
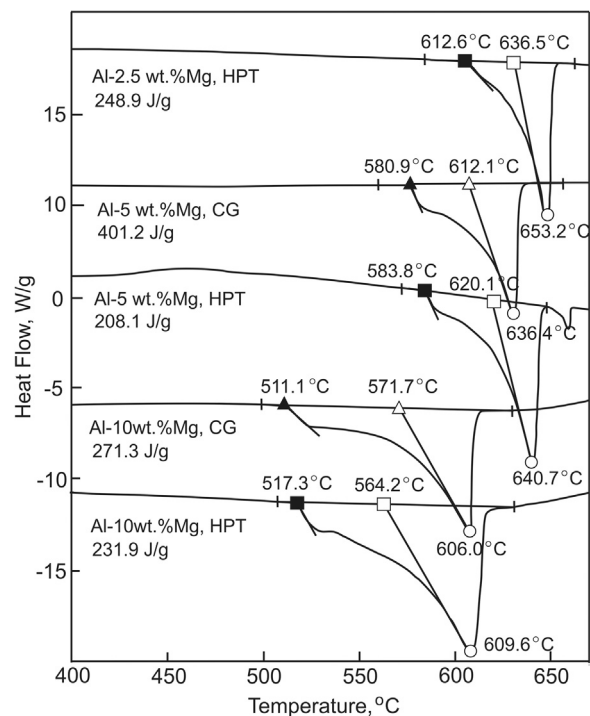
Fig. 2. Temperature dependence of heat flow (DSC curves) for the Al−Mg samples: ○, liquidus temperature; ▲, incomplete wetting of GB for coarse-grained alloys; ■, incomplete wetting of GB for fine-grained (HPT) alloys; Δ, complete wetting of GB for coarse-grained alloys; □, complete wetting of GB for fine-grained (HPT) alloys.

2. Experimental

The Al alloys with 2.5, 5 and 10 wt% Mg were prepared of high purity components (99.999% Al and 99.99% Mg) by vacuum induction melting. As-cast disks of these alloys obtained after sawing, grinding and chemical etching were subjected to HPT at room temperature under the pressure of 5 GPa in a Bridgman anvil type unit (5 torsions, duration of process about 300 s) [40–42]. All samples for structural and calorimetric investigations were cut from the deformed disks at a distance of 3 mm from the sample centre. DSC measurements were performed using the TA Instruments 910 and 1600 calorimeters. Transmission electron microscopy (TEM) investigations were carried out using a TECNAI G2 F20 microscope at an accelerating voltage of 200 kV.

3. Results and discussion

In Fig. 1a the bright field TEM micrograph is shown for the Al−10 wt% Mg alloy after HPT and one 20−400 °C heating cycle in DSC calorimeter. The average grain size of (Al) solid solution increased from 90 nm before heating cycle to about 500 nm after heating up to 400 °C. The alloy contains grains of (Al) solid solution with small particles of β-phase (Al_3Mg_2) in GBs. It is completely recrystallized, the higher elastic energy stored in the HPT-processed samples as compared to the as-cast almost dislocation-free samples fully relaxed after heating. The only remained difference is the smaller grain size of HPT-treated samples. The average (Al) grain size in the as-cast Al−10 wt% Mg alloy after heating from 20 to 400 °C in DSC remains the same (about 50 μm) (Fig. 1b). The microstructure shown in Fig. 1 was the starting point for the high-temperature DSC experiments.

Fig. 2 shows DSC curves for the Al−Mg samples with 2.5, 5 and

10 wt% Mg for heating from 20 to 670 °C at a rate of 10 K min⁻¹. Only the high-temperature part between 400 and 670 °C is shown. For the Al−Mg alloys with 5 and 10 wt% Mg, curves for both as-cast coarse-grained and fine-grained HPT-samples are shown. According to the standard approach to the quantification of DSC curves of the alloys melting between solidus and liquidus temperatures [43] (these procedures are also included in the quantification software of modern DSC equipment), the position of a deep minimum corresponds to the end of melting, i.e. to the liquidus temperature (open circles in Fig. 2). The measured minima positions for all samples correspond well to the literature data for the liquidus in the Al−Mg bulk phase diagram (Fig. 3 [44]). In the standard case [43], the left side of the DSC minima for the
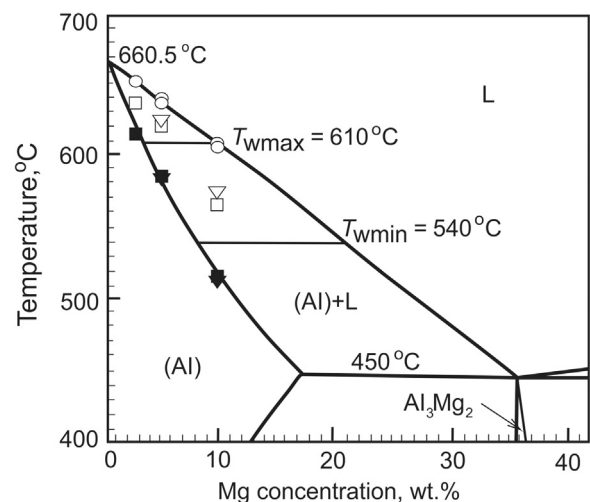

Fig. 3. Part of the Al−Mg phase diagram. Thick lines mark the bulk liquidus and solidus [44]. Experimental points are taken from Fig. 2: ○, liquidus temperature; ▲, incomplete wetting of GB for CG alloys; ■, incomplete wetting of GB for fine-grained (HPT) alloys; Δ, complete wetting of GB for CG alloys; □, complete wetting of GB for fine-grained (HPT) alloys.

melting follows the linear tangent almost until the intersection point with the base line. In this work (Figs. 2 and 3), each of DSC curves deviates from this tangential. The temperatures given by the conventional procedure (i.e., defined using the intersection of the baseline and the tangential to the left side of the minimum) lie deep in the middle between solidus and liquidus lines (open squares and open triangles in Figs. 2 and 3) [45,46]. A kind of broad "shoulder" is visible in the left part of each melting minimum. Even more, the presence of a secondary, superimposed, peak (itself with a minimum) may be guessed from the Figs. 2 and 3 for both as-cast coarse-grained and fine-grained HPT-samples. Such "shoulder" is more visible in Fig. 2 for Al–10 wt% Mg alloy. These "shoulders" positions to the left of the main DSC minimum reveal the second weak melting process in the samples. It is possible to draw the second tangential at the lower temperature in comparison with the "main" melting tangential (Figs. 2 and 3). The temperatures obtained by the intersection of second tangential with a base line are now close to the values of solidus temperatures (full squares and full triangles in Fig. 3) [45,46].

It was supposed that this two-stage melting is due to the transition from incomplete to complete wetting of GBs by the melt. Such transition was observed both in binary Al–Zn and ternary Al–Zn–Mg alloys [8,45,47]. During conventional melting, the bulk phase gradually becomes liquid between solidus and liquidus lines. In this case, the tangential to the left side of the DSC melting curve intersects the base line almost in the point where the DSC melting curve starts to come down from the base line. In case of GB wetting, the first portions of melted bulk redistribute along GBs in order to wet them and to separate the remaining solid grain one from another. The heat of the melting also redistributes to the lower temperatures, the shape of the DSC melting curve changes, and the tangential shifts to the higher temperature from the bulk solidus (Figs. 2 and 3). The shape change of the DSC curve depends on the GB energy spectrum and, therefore, on the spectrum of GB wetting temperatures T_w. In the extreme case, if the T_w temperatures group close to the solidus point, the "shoulder" in melting curve is rather pronounced (like for Al–10 wt% Mg in Fig. 2). If the T_w temperatures are uniformly distributed, the "shoulder" in melting curve is less pronounced (like for Al–2.5 wt% Mg and Al–5 wt% Mg in Fig. 2), and only the shift of the tangential with the base line indicates the GB melting effect. Thus, when the Al–2.5 wt% Mg and Al–5 wt% Mg alloys starts to melt, many GBs should become completely wetted at once. The heat of this GB wetting process is localized in the narrow temperature interval slightly above the solidus temperature. For the Al–10 wt% Mg alloy, the solidus temperature is lower than the minimum temperature of the wetting transition T_{wmin}=540 °C, and the liquidus temperature is close to the maximum temperature of the wetting transition T_{wmax}=610 °C (Fig. 3). This means that all GBs become completely wetted between the solidus and liquidus temperatures, one after another. As a result, the "shoulder" in the melting curve for the Al–10 wt% Mg alloy is broader than that for the Al–5 wt% Mg and Al–2.5 wt% Mg alloys.

In Al–Zn alloys we observed that the melting starts ~10–25 °C below the bulk solidus line [37]. It means that between GB solidus (premelting) line and bulk solidus the GB contains the layer of a liquid-like phase [14,16,17,21,22,25,27,48]. Such layers could ensure the extremely high superplasticity of Al-based alloys just below the bulk solidus line [47]. However, in ternary Al–Zn–Mg alloys the melting starts almost exactly at the bulk solidus line [39]. In this work (Figs. 2 and 3) we also see that the GB solidus line for Al–Mg alloys is very close to the bulk solidus (no more than 2 °C lower). It means that, most probably, the addition of magnesium to the Al-based alloys makes the area between GB and bulk solidus narrower.

4. Summary and conclusions

1. The transition from incomplete to complete GB wetting in binary Al–Mg alloys manifests itself in the asymmetric shape of the melting curve measured by DSC.

2. The shape of the "shoulder" in the melting curve depends on the position of GB wetting tie-lines between the solidus and liquidus temperatures.

3. In the contrast to the Al–Zn alloys, the GB solidus line for Al–Mg alloys is very close to the bulk solidus. The difference between them does not exceed 2 °C.

References

[1] M. Furukawa, Z. Horita, M. Nemoto, et al., Acta Mater. 44 (1996) 4619–4629.
[2] A.A. Mazilkin, B.B. Straumal, E. Rabkin, et al., Acta Mater. 54 (2006) 3933–3939.
[3] H.-J. Lee, J.-K. Han, S. Janakiraman, et al., J. Alloy. Compd. 686 (2016) 998–1007.
[4] P. Bazarnik, Y. Huang, M. Lewandowska, et al., Mater. Sci. Eng. A 626 (2015) 9–15.
[5] A.A. Khamei, K. Dehghani, Mater. Sci. Eng. A 627 (2015) 1–9.
[6] H.J. Roven, M. Liu, M.Y. Murashkin, et al., Mater. Sci. Forum 604-605 (2008) 179–186.
[7] Z. Lee, F. Zhou, R.Z. Valiev, et al., Scr. Mater. 51 (2004) 209–214.
[8] B.B. Straumal, G. López, E.J. Mittemeijer, et al., Def. Diff. Forum 216 (2003) 307–312.
[9] B.B. Straumal, B. Baretzky, O.A. Kogtenkova, et al., J. Mater. Sci. 45 (2010) 2057–2061.
[10] M. Fatmi, F. Sahnoune, H. Belhouchet, et al., Chin. J. Phys. 54 (2016) 216–222.
[11] L. Liu, D. Ren, F. Liu, Mater 7 (2014) 3735–3757.
[12] J.W. Cahn, J. Chem. Phys. 66 (1977) 3667–3676.
[13] C. Ebner, W.F. Saam, Phys. Rev. Lett. 38 (1977) 1486–1489.
[14] B.B. Straumal, W. Gust, Mater. Sci. Forum 207 (1996) 59–68.
[15] B.B. Straumal, W. Gust, T. Watanabe, Mater. Sci. Forum 294 (1999) 411–414.
[16] W.D. Kaplan, D. Chatain, P. Wynblatt, et al., J. Mater. Sci. 48 (2013) 5681–5717.
[17] P.R. Cantwell, T. Ming, S.J. Dillon, et al., Acta Mater. 62 (2014) 1–48.
[18] P. Bueno, J. Varela, E. Longo, J. Eur. Ceram. Soc. 28 (2008) 505–529.
[19] J. Luo, Y.M. Chiang, R.M. Cannon, Langmuir 21 (2005) 7358–7365.
[20] D.R. Clarke, J. Am. Ceram. Soc. 70 (1987) 15–22.
[21] J. Luo, Crit. Rev. Solid State Mater. Sci. 32 (2007) 67–109.
[22] E.I. Rabkin, L.S. Shvindlerman, B.B. Straumal, Int. J. Mod. Phys. B 5 (1991) 2989–3028.
[23] J. Luo, Y.M. Chiang, Ann. Rev. Mater. Res. 38 (2008) 227–249.
[24] B.B. Straumal, A.S. Gornakova, O.A. Kogtenkova, et al., Phys. Rev. B 78 (2008) 054202.
[25] A. Subramaniam, C. Koch, R.M. Cannon, et al., Mater. Sci. Eng. A 422 (2006) 3–18.
[26] I. Maclaren, Ultramicroscopy 99 (2004) 103–113.
[27] D. Bonn, D. Ross, Rep. Prog. Phys. 64 (2001) 1085–1163.
[28] R.Z. Valiev, M.Y. Murashkin, A. Kilmametov, et al., J. Mater. Sci. 45 (2010) 4718–4724.
[29] B.B. Straumal, B. Baretzky, A.A. Mazilkin, et al., Acta Mater. 52 (2004) 4469–4478.
[30] A.A. Mazilkin, O.A. Kogtenkova, B.B. Straumal, et al., Def. Diff. Forum 237 (2005) 739–744.
[31] A.A. Mazilkin, B. Baretzky, S. Enders, et al., Def. Diff. Forum 249 (2006) 155–160.
[32] B.B. Straumal, X. Sauvage, B. Baretzky, et al., Scr. Mater. 70 (2014) 59–62.
[33] B. Sulkowski, A. Panigrahi, K. Ozaltin, et al., J. Mater. Sci. 49 (2014) 6648–6655.
[34] K. Edalati, Z. Horita, Mater. Sci. Eng. A 652 (2016) 325–352.
[35] S.V. Divinski, J. Ribbe, G. Reglitz, et al., J. Appl. Phys. 106 (2009) 063502.
[36] X. Sauvage, Y. Champion, R. Pippan, et al., J. Mater. Sci. 49 (2014) 5640–5645.
[37] B. Straumal, R. Valiev, O. Kogtenkova, et al., Acta Mater. 56 (2008) 6123–6131.
[38] B.B. Straumal, A. Korneva, O. Kogtenkova, et al., J. Alloy. Compd. 615 (2014) S183–S187.
[39] B.B. Straumal, O.A. Kogtenkova, S.G. Protasova, et al., J. Mater. Sci. 46 (2011) 4243–4247.
[40] R. Valiev, R. Islamgaliev, I. Alexandrov, Prog. Mater. Sci. 45 (2000) 103–189.
[41] K. Yang, Yu Ivanisenko, A. Caron, et al., Acta Mater. 58 (2010) 967–978.
[42] W. Skrotzki, A. Eschke, B. Jóni, et al., Acta Mater. 61 (2013) 7271–7284.
[43] J.A. Dean, The Analytical Chemistry handbook, McGraw Hill, New York, 1995, p. 151 (Standards ASTM D 3417, ASTM D 3418, ASTM E 1356, ISO 11357).
[44] T.B. Massalski (Ed.)Binary Alloy Phase Diagrams, ASM International, Materials

Park, OH, 1990.

[45] B.B. Straumal, O. Kogtenkova, P. Zięba, Acta Mater. 56 (2008) 925–933.

[46] O.A. Kogtenkova, S.G. Protasova, A.A. Mazilkin, et al., J. Mater. Sci. 47 (2012) 8367–8371.

[47] B. Straumal, G. López, W. Gust, et al., Effect of the grain boundary phase transitions on the superplasticity in the Al–Zn system, in: M.J. Zehetbauer, R.Z. Valiev (Eds.), Nanomaterials by Severe Plastic Deformation: Fundamentals, Processing, Applications, John Wiley, VCH, Weinheim, 2004, pp. 642–647.

[48] L.-S. Chang, E. Rabkin, B.B. Straumal, et al., Def. Diff. Forum 156 (1998) 135–146.